RSC Advances

Nacre-Mimetic Epoxy Matrix Composites Reinforced by Two-Dimensional Glass Reinforcements

Journal:	*RSC Advances*
Manuscript ID	RA-ART-11-2015-025049.R2
Article Type:	Paper
Date Submitted by the Author:	04-Mar-2016
Complete List of Authors:	Gurbuz Guner, Selen; Middle East Technical University, Department of Metallurgical and Materials Engineering Dericioglu, Arcan; Middle East Technical University, Department of Metallurgical and Materials Engineering
Subject area & keyword:	Composites < Materials

Journal Name

ARTICLE

Nacre-Mimetic Epoxy Matrix Composites Reinforced by Two-Dimensional Glass Reinforcements

S. N. Gurbuz Guner[a] and A. F. Dericioglu*[a]

Received 00th January 20xx,
Accepted 00th January 20xx

DOI: 10.1039/x0xx00000x

www.rsc.org/

Inspired by the micro-scale "brick-and-mortar" architecture of nacre, epoxy matrix composites reinforced by aligned two-dimensional glass reinforcements were fabricated using a newly proposed simple, one-step, time and man-power efficient processing pathway called Hot-press Assisted Slip Casting process (HASC). Effect of reinforcement aspect ratio along with interfacial compatibility and bonding on mechanical behavior of the fabricated bulk nacre-mimetic composites was investigated. Achieved results indicated that composites reinforced by high aspect ratio flakes exhibited high energy absorption values until fracture as a result of extensive crack deflection along with flake pull-out leading to highly torturous crack path similar to the crack growth behavior of natural nacre. Furthermore, functionalization of the reinforcement surfaces by silane coupling agent improved the compatibility and interfacial adhesion between the reinforcements and the matrix resulting in considerable enhancement of mechanical properties of fabricated bulk lamellar composites.

1. Introduction

Nacre, the mother-of-pearl, being one of the most intriguing natural materials, consists of 95 vol% inorganic platelets (aragonite) and 5 vol% organic biopolymer. Despite its high brittle inorganic content, this fascinating natural material reveals enhanced mechanical characteristics including unique toughness and mechanical strength combination [1-3]. This extraordinary combination of mechanical properties makes nacre the "bio-mimetic model" and the source of inspiration in many studies. For that reason, intensive research has been devoted to understand the structure-property relationship and to explore the underlying design principles found in nacre. The main reason underlying the distinct combination of high strength, stiffness and toughness is thought to be the micro-scale "brick-and-mortar" architecture spanning over several length scales along with the nano- and micro-scale intriguing interfacial features each of which is suggested to undertake a certain task and operate synergistically [4-10].

Even though the investigations explicitly pointed out the multi-scale complex architecture of nacre as the reason of its outstanding mechanical performance, replication of this multi-scale hierarchical structure and all key features of nacre is a difficult task using the current technology [1]. For this reason, the bio-inspiration studies mainly focused on mimicking the micro-scale "brick-and-mortar" structure of nacre [11, 12].

Layer-by-layer assembly [13-17], vacuum filtration-induced self-assembly (or paper-making process) [18-20], water evaporation-induced self-assembly (or solution casting) [21-23] and tape casting (doctor-blading) [24-27] are the most widely used techniques to fabricate composites with nacre-mimetic "brick-and-mortar" structure. Even though all of these processes are effective in fabricating strong and though bio-inspired self-standing films or coatings exhibiting hierarchical architectures, they cannot be used to fabricate nacre-like bulk composites.

In recent years, ice-templating or so-called freeze casting method [28-30], gel casting and hot-pressing [31, 32] as well as various flake powder metallurgy routes [33-35] and magnetic alignment [36, 37] have been proposed to fabricate nacre-mimetic bulk composites. Although, all of these proposed techniques are relatively simple, most of them are multi-step and time-consuming. Consequently, there is still need for a simple, one-step, scalable, time and man-power efficient processing strategy which enables the fabrication of bulk composites reinforced by well-aligned 2D reinforcements in high volume fractions that can be used in large scale components.

Current study focused on the design and fabrication of nacre mimetic two-dimensional (2D) glass reinforcement-epoxy matrix composites using a newly proposed simple, one-step, time and man-power efficient processing pathway called "Hot-press Assisted Slip Casting (HASC)". To investigate the effect of reinforcement aspect ratio on mechanical properties of the nacre-mimetic composites, epoxy matrix was reinforced by micron-thick low aspect ratio glass platelets along with high aspect ratio glass flakes. Considering the design principle that successfully describes the relationship between the micro-scale "brick-and-mortar" structure and the mechanical properties of natural nacre [3], glass platelets and flakes with an

[a] Department of Metallurgical and Materials Engineering, Middle East Technical University, Universiteler Mah. Dumlupinar Bulv. No: 1, 06800 Ankara, Turkey. E-mail: arcan@metu.edu.tr

aspect ratio lower than the critical value, for the present glass reinforcement-epoxy matrix system, were selected to ensure that the failure would be governed by platelet pull-out mode. To achieve interfacial compatibility along with improved adhesion and to reveal the effect of interfacial strength on the mechanical performance of the nacre-mimetic inorganic-organic composites, the surfaces of the glass reinforcements were treated with epoxy compatible amino functional silane coupling agent to impart interfacial bonding between the organic matrix and the 2D inorganic reinforcements.

2 Experimental

2.1 Materials

Throughout this study, two-dimensional (2D) glass reinforcements with different aspect ratios were used. These reinforcements were classified as glass platelets (GP) or glass flakes (GF) on account of their aspect ratios [38]. Aspect ratio of modified C-glass platelets (ECR GF003, average diameter of <50 μm and thickness of 2.3-3.3 μm, Glass Flake Ltd., Leeds, UK) and C-glass flakes (RCF2300, average diameter of 300 μm and thickness of 2 μm, Nippon Sheet Glass Co. Ltd., UK) are ~15-20 and ~150, respectively. As the matrix material, low viscosity Diglycidyl Ether of Bisphenol-A (DGEBA) containing epoxy resin and hardener (Triethylenetetramine) was used (EpoFix, Struers GmbH, Germany).

2.2 HASC Processing of Nacre-Mimetic Inorganic-Organic Composites

For the fabrication of nacre-mimetic composites, inorganic reinforcements, either as-received or surface functionalized, were mixed with epoxy resin and hardener (Resin/hardener ratio: 25/3 by weight) at 2000 rpm using a planetary centrifugal homogenizing mixer. In the final mixture, volume fraction of glass reinforcements was ~20 vol%. Prepared glass reinforcement-epoxy slurry was poured into the steel die having a rectangular inner cavity of 20 by 27 mm, and hierarchical arrangement of the 2D reinforcements in the epoxy matrix was achieved through the novel technique called “Hot-press Assisted Slip Casting (HASC)”. In this technique, a porous plaster was cast into a rectangular cross-sectioned steel die before processing. Then, prepared inorganic reinforcement-epoxy mixture was poured into the die inner cavity. Die assembly was then placed in a conventional hydraulic hot-press, temperature of which had been set to 50°C, and initial pressure was applied until resin flow initiates through the porous plaster from underneath the steel die. Following this, pressure was increased gradually (~5 MPa/min) until the desired pressure level was reached. After ~15-20 min later than the starting of the processing, temperature of the temperature of the system was also increased to 120 °C with a rate of 3-3.5°C/min. Finally, the system was kept at 120 °C for 20 min under the applied pressure to cure the epoxy matrix. Schematic illustration of the HASC processing pathway is shown in Figure 1. In this novel processing pathway, porous plaster functions as a filter draining the excess resin and aids in increasing the reinforcement content together with the alignment of the 2D reinforcements by the flow of the resin during the hot-pressing process.

In this study, nacre-mimetic composites reinforced either by low aspect ratio glass platelets or high aspect ratio glass flakes were fabricated using this novel processing technique. Optimization of HASC processing pressure and investigation of its effect on the microstructural architecture of the composites were performed in glass platelet-epoxy system due to the lower in-plane dimension and thickness of the glass platelets (GP) as compared to those of the glass flakes (GF). To reveal the effect of platelet alignment and volume fraction on the improvement of the mechanical properties, neat epoxy as well as simple mixed (SM) samples (as-mixed and cured without applying pressure) were also processed as control samples applying the same curing cycle. After the determination of the optimum hot-pressing pressure, nacre-mimetic composites reinforced by high aspect ratio glass flakes were also fabricated.

2.3 Surface Functionalization of Glass Reinforcements

To achieve compatibility and interfacial bonding between inorganic reinforcements and organic matrix, surfaces of the glass platelets and flakes were functionalized with amino-functional silane coupling agent, γ-aminopropyltriethoxysilane (APS, Silquest A-1100, Momentive Performance Materials Inc., Ohio, USA). Toluene was used as the solvent based on the results of our previous study [39]. Chemical structure of the used organofunctional silane and details of the surface functionalization procedure can be found elsewhere [39]. After functionalization with silane coupling agent, surface treated glass platelets and flakes were used to fabricate nacre-mimetic epoxy matrix composites using above described HASC processing technique applying the pre-determined optimum pressure.

Journal Name

ARTICLE

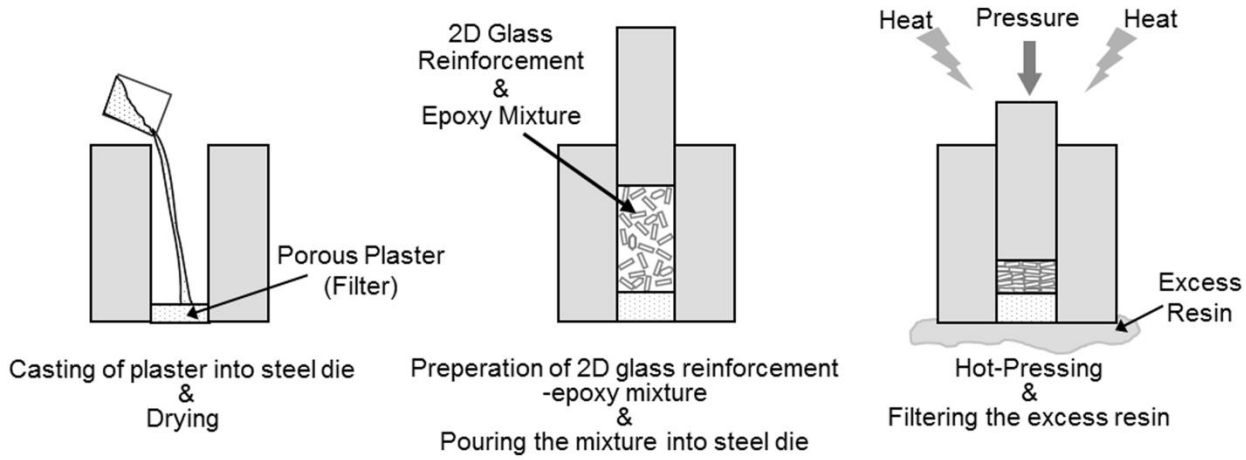

Figure 1 Schematic illustration of Hot-press Assisted Slip Casting (HASC) processing pathway.

2.4 Characterization

Reinforcement content of the composite samples (wt %) was determined by physically removing the epoxy matrix by combustion and weighing the inorganic residue (GP or GF). The volume fraction of the inorganic reinforcement was calculated using determined weight percentage values, known density of glass reinforcements and density of neat epoxy which was measured by the Archimedes' principle. Microstructural characterization was conducted by examining polished (mounted in epoxy resin, ground and polished down to 0.5 μm diamond suspension) and fracture surfaces of the specimens under scanning electron microscope (SEM) (FEI Nova Nano SEM 430). Vickers hardness measurements were carried out using microhardness tester (HMV 2 E, Shimadzu, Kyoto, Japan) with an applied maximum load of 0.5 kg for 10 seconds. Flexural strength, strain and modulus of the composites were measured by three-point bending tests. Length (l), width (b) and thickness (d) of the three-point bending specimens were 20, 5 and 1 mm, respectively. Tests were conducted with a span length of 16 mm and cross-head speed of 0.4 mm/min. For both Vickers hardness measurements and three-point bending tests applied loading direction was parallel to hot-pressing direction. Surface functionalization of the glass reinforcements with silane coupling agents was characterized by X-ray photoelectron spectroscopy (XPS) (PHI 5000 Versa Probe). XPS analyses of both as-received and silane-treated glass reinforcements were carried out using monochromatic Al Kα radiation source. XPS survey spectra were collected with pass energy of 187.85 eV at a photoelectron take-off angle of 45°. High resolution XPS spectra of N1s core levels were acquired with pass energy of 58.70 eV. Peak deconvolution of N1s core levels was performed using mixed Gaussian-Lorentzian function after the subtraction of Shirley background.

Effect of microstructural architecture and interfacial bonding on the crack growth behavior and energy required for fracture was investigated through work of fracture (WOF) tests. The specimens with single edge notch beam (SENB) geometry were tested with a span of 16 mm and cross-head speed of 0.05 mm/min. Length (l), width (b) and thickness (d) of the work of fracture test specimens were 20, 3 and 4 mm, respectively. The span (S)/thickness (d) ratio was kept as 4 to facilitate stable fracture [3]. The notch, with a size of 0.45d-0.55d, was machined with diamond saw and a sharp pre-crack was introduced by sliding a fresh razor blade across the notch. WOF value for each specimen was calculated using the following equation where E is area under the load-displacement curve and A is the fracture surface area of the specimen.

$$WOF = E/2A$$

In WOF method, fracture surface area is taken as cross-sectional area of fracture surface assuming that it is smooth. However, actual fracture surfaces are generally rough, especially for composites reinforced with 2D reinforcements that fail under platelet pull-out mode as in the case of natural nacre. Therefore, use of cross-sectional fracture surface area may lead to overestimation of fracture energies. Despite this fact, this approach has been widely used to characterize the mechanical properties of natural nacre [3, 40, 41] and also bio-inspired nacre-like composites [34, 42, 43].

3. Results and Discussion

3.1 Inorganic–Organic Nacre-Mimetic Composites with As-received Glass Platelets

"Hot-press Asisted Slip Casting" processing pathway, being a one-step, easy, fast and effective processing methodology, is a promising technique that enables the fabrication of nacre-mimetic bulk composites with high inorganic content. In this process, the excess resin is forced to flow through a porous plaster under the action of applied hot-pressing pressures, resulting in an increase in the volume fraction of inorganic reinforcements, i.e. even the application of the lowest pressure 25 MPa leads to 2.5 fold increase in the glass platelet content with respect to SM composite proving the effectiveness of HASC processing in increasing the total inorganic volume fraction (Figure 2).

In our previous study that focused on the fabrication of alumina platelet-epoxy nacre-mimetic composites, HASC processing has proved its efficiency in the alignment of sub-micron thick alumina platelets, with an aspect ratio, α, of ~33, leading to "brick-and-mortar" like arrangement [39]. However, for glass platelet-epoxy system, SEM images (Figure 3) indicate that although alignment of the platelets is favored by the drainage of the epoxy resin during HASC processing, misalignment sites also exist.

Three-point bending test results of the fabricated epoxy matrix composites indicated that incorporation of glass platelets has led to a decrease in both flexural strength and strain values of the neat epoxy (

Table **1**). For the SM sample, incorporation of 20 vol% glass platelet with random orientation into epoxy matrix results in ~22% reduction in flexural strength. Reinforcing the epoxy with ~56 vol% aligned glass platelets through HASC processing, which is 2.7 fold higher than the inorganic content of the SM composite, has led to a decrease of only ~4% in flexural strength with respect to SM composite. However, further increase in the inorganic content resulted in a more dramatic decrease in the flexural strength ranging between 44-57% and 28-45% with respect to neat epoxy and SM composite, respectively.

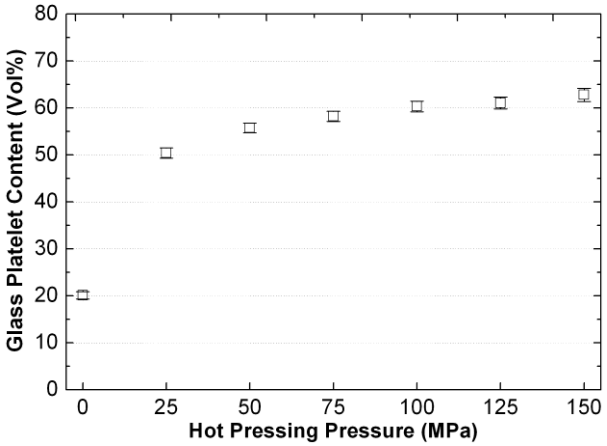

Figure 2 Glass platelet content of the HASC processed composites as a function of hot pressing pressure along with the glass platelet content of SM sample (0 MPa).

The decrease in the flexural strength with the incorporation of glass platelets, even for the low amount of inorganic containing SM composite, can be attributed to the lack of coupling between the platelets and the epoxy matrix along with the presence of voids at the interface (shown with white arrows in Figure 3) leading to a decrease in the stress transfer from matrix to the reinforcement. Dramatic decrease in the flexural strength for the composites HASC processed with an applied pressure of 75 MPa and higher is thought to be arisen from the increase in the number of fractured platelets along with the increase in the size of the platelet clusters, in which platelets are stacked together with insufficient epoxy between them, leading to further reduction in the effective load transfer (Figure 3). Furthermore, as the size of these clusters increases and reaches to a critical value formed clusters are thought to act as stress concentration sites. Rigid glass platelets were probably fragmented into two or more pieces during HASC processing with a concomitant reduction in the aspect ratio.

Table 1 Mechanical properties of the SM and HASC processed composites reinforced with as-received platelets along with the mechanical properties of neat epoxy.

Designation	Hot Pressing Pressure (MPa)	Inorganic Content (Vol %)	Flexural Strength (MPa)	Failure Strain	Flexural Modulus (GPa)	Hardness (HV 0.5)
Neat Epoxy	0	0	103.3±2.2	0.10271±0.00256	2.4±0.1	19.6±0.6
SM	0	20±0.8	80.8±2.1	0.02098±0.00151	4.3±0.1	25.2±1.2
GP-HASC 25	25	50±1.1	75.6±1.8	0.00972±0.00019	9.0±0.1	39.5±1.2
GP-HASC 50	50	56±1.0	77.6±2.6	0.00937±0.00022	9.9±0.2	47.0±1.9
GP-HASC 75	75	58±1.1	58.4±2.0	0.00915±0.00045	7.7±0.3	42.1±1.2
GP-HASC 100	100	60±1.1	56.5±1.3	0.00868±0.00008	7.7±0.4	36.6±1.1
GP-HASC 125	125	61±1.2	51.7±1.4	0.00828±0.00049	7.1±0.4	34.6±1.6
GP-HASC 150	150	63±1.4	44.3±2.0	0.00784±0.00035	6.5±0.4	30.9±2.8

Journal Name

ARTICLE

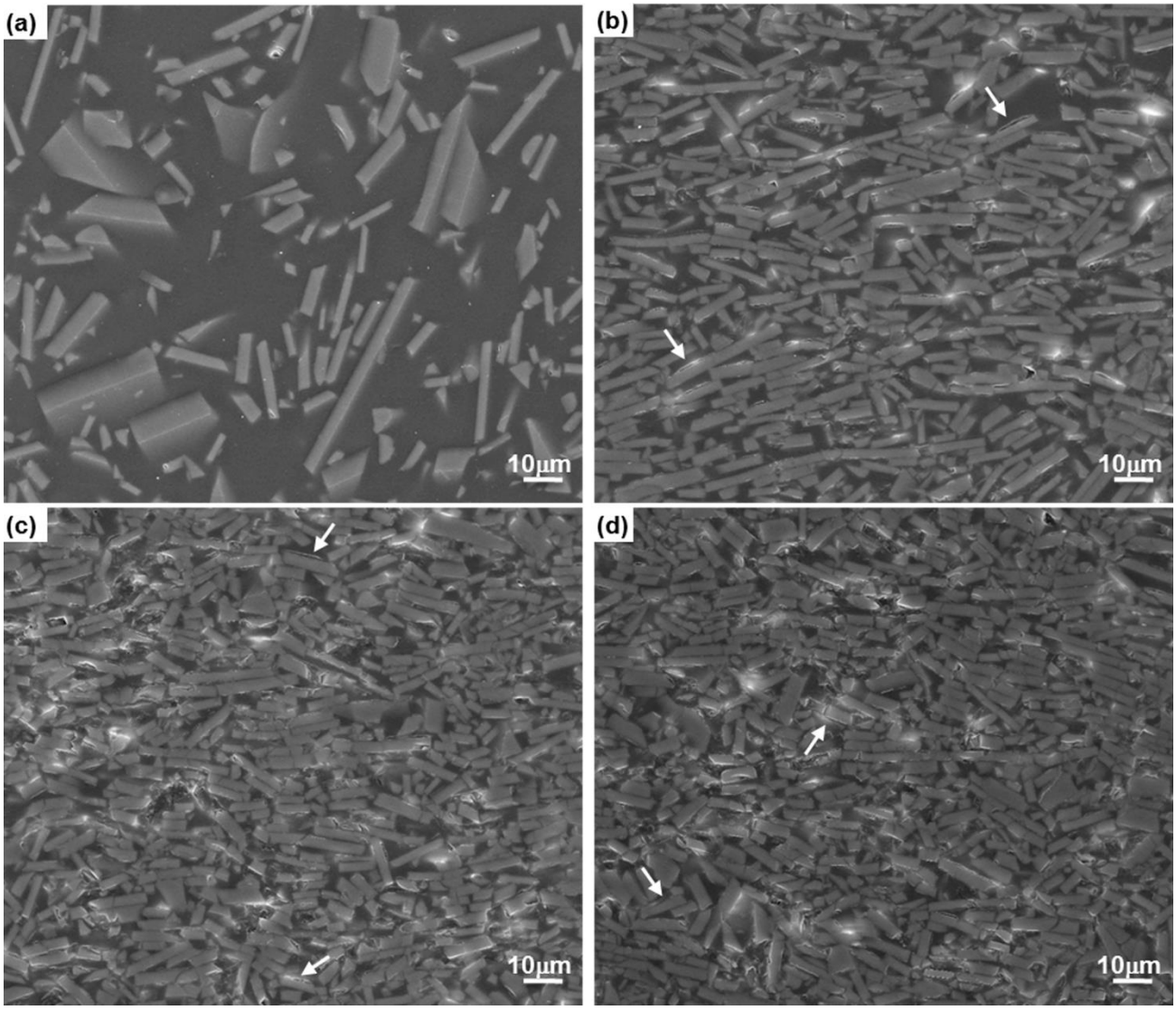

Figure 3 Cross-sectional microstructure of (a) SM and HASC processed composites for the applied pressures of (b) 50 MPa, (c) 100 MPa and (d) 150 MPa.

On the other hand, incorporation of rigid glass platelets into the epoxy matrix has led to an increase in both flexural modulus and hardness with respect to neat epoxy (
Table **1**). In the case of SM composite, incorporation of 20 vol% glass platelets resulted ~2 and ~1.3 fold enhancements in flexural modulus and hardness, respectively. For the HASC processed composites, the increase in inorganic content along with the alignment of the platelets has led to further increase in flexural modulus and hardness values up to a glass content of 56 vol%, above which further increase in platelet content have caused a decrease in both values. This decrease in the flexural modulus through HASC processing, after ~4 and ~2.3 fold increases with respect to neat epoxy and SM composite, can be attributed to the decrease in the effective aspect ratio which is caused by the fragmentation of the platelets and increase in the size of the platelet clusters leading to a decrease in the efficiency of rigid 2D fillers in restricting the deformation of the matrix. Figure 4 shows the fracture surfaces of the three-point bending (3PB) tested SM and HASC processed composite under the applied processing pressure of 50 MPa. From this figure it is evident that fracture occurs through platelet/matrix interface leaving the platelet surfaces

smooth indicating the lack of adhesion between the platelets and the matrix. Platelet debonding (shown with black arrows) and smooth platelet pull-out sites (shown with white arrows) reveal that the fracture mechanism is mainly governed by platelet debonding and platelet pull-out for these composites rather than platelet fracture.

3.2 Inorganic–Organic Nacre-Mimetic Composites with As-received Glass Flakes

The relationship between brick-and-mortar structure of nacre and the resultant mechanical properties is best described by the simple shear lag model [3]. According to this model, the aspect ratio of the discontinuous 2D reinforcements should be as high as possible in order to increase the stress transfer lengths and to utilize the strength potential of the reinforcements with maximum efficiency, yet lower than a critical value to ensure that the fracture is governed by reinforcement pull-out mode rather than reinforcement fracture [3, 44].

For the present glass reinforcement-epoxy matrix composite system, the critical aspect ratio, which is equal to tensile strength of platelet/flake (σ_p) divided by yield shear strength of the matrix (τ_m), can be calculated by assuming the tensile strength value of C-glass flake/platelet as 3.4 GPa [45]. The value of the matrix yield shear strength for the Bisphenol A-diglycidyl ether (DGEBA) based epoxy system that was used in this study has not been reported by the manufacturer. Therefore, as a preliminary approach, matrix yield shear strength value is taken as ~15 MPa based on the reported matrix yield shear strength value of another DGEBA based epoxy resin [46]. In view of these, critical aspect ratio was determined as ~225 for 2D glass reinforcement–epoxy matrix system. Considering this design principle, chemically resistant C-glass flakes with an aspect ratio (α) of 150 were chosen and used to reinforce the epoxy matrix to increase stress transfer lengths, and hence strengthening efficiency while ensuring that the governed fracture mode is not platelet fracture which leads to catastrophic failure. To compare the results with those of the composites reinforced by low aspect ratio C-glass platelets, the volume fraction of the flakes were kept as 20 vol% in the initial mixture. Glass flake reinforced composites were fabricated by HASC processing under the applied pressure of 50 MPa, which has led to the optimum results in the case of glass platelet reinforced composites. In addition to this, 100 MPa was also applied to reveal the effect of higher processing pressures. For the SM composite, incorporation of 20 vol% high aspect ratio glass flakes rendered the initial mixture so viscous that the elimination of air bubbles became impossible as hot-pressing was not applied on this sample. For this composite, the results of the mechanical characterization studies are not be presented here as they are not reliable because of the very large bubbles that were entrapped.

For the HASC processed glass flake reinforced composites, applied pressures of 50 MPa and 100 MPa have led to excessive drainage of the epoxy resin through the porous filter leading to composites containing ~76 vol% and ~78 vol% high aspect ratio glass flakes, respectively. It is interesting to note that there is 20 vol% difference in the inorganic content of the composites reinforced by glass platelets and glass flakes under the identical applied processing pressures. Beside their higher inorganic 2D reinforcement content, preferential alignment of high aspect ratio glass flakes were also successfully achieved via HASC processing. Cross sectional view of HASC processed composite under the applied pressure of 50 MPa, shown in Figure 5, illustrates the micro scale nacre-mimetic structure of the high aspect ratio glass flake reinforced composite.

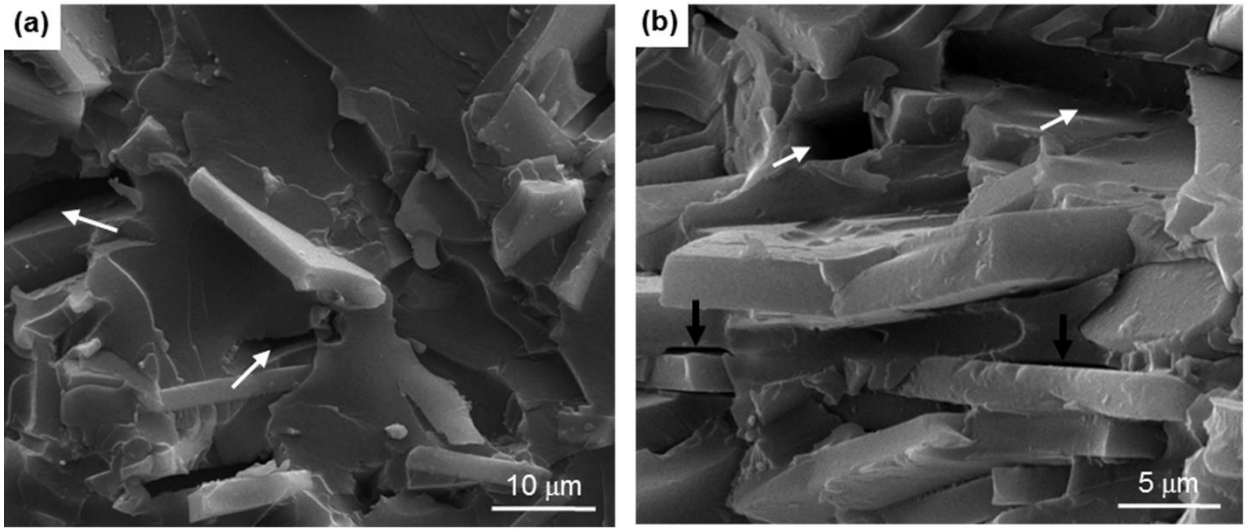

Figure 4 SEM images showing the fracture surfaces of (a) SM and (b) HASC processed composite under the applied pressure of 50 MPa.

The efficiency of HASC processing pathway in fabricating composites with an architecture resembling to "brick-and-mortar" structure of natural nacre may be explained based on

the Onsager Theory [47]. According to this theory, in suspensions of hard asymmetric 2D colloidal particles such as plates and rods, phase transition from orientationally disordered isotropic (I) phase to the ordered nematic phase (N) may occur. This phase transition is driven by packing entropy or excluded volume as a function of increase in the volume fraction of 2D particles [47, 48]. In the present processing pathway, forcing the liquid resin to flow through the porous plaster leads to an increase in the volume fraction of the 2D inorganic reinforcement in the 2D inorganic reinforcement – liquid organic mixture. As a result of the increase in the inorganic concentration, the tendency of platelets/flakes for alignment increases to reduce the excluded volume, and hence to increase the entropy of the system. Furthermore, flow of the resin through the randomly oriented 2D reinforcements also aids in rearrangement of the reinforcements to more favorable configuration by transferring kinetic energy.

The critical volume fraction of 2D particles required for I-N phase transition has strong dependence on aspect ratio of the 2D particles. Plates/rods with higher aspect ratios show more tendency for orientational ordering and, therefore, I-N phase transition occurs at lower 2D particle concentrations [48, 49]. Comparison of the cross sectional views of the HASC processed composites reinforced with glass platelets (Figure 3), glass flakes (Figure 5) and alumina platelets [39] explicitly illustrates this fact, i.e., the tendency for alignment through HASC processing increases with the increase in aspect ratio of the 2D inorganic reinforcement. For instance, in the case of composites reinforced with almost the same fraction of inorganic platelets, HASC processing is more effective in aligning alumina platelets (α=~33) than glass platelets (α=~15-20). On the other hand, best alignment was achieved in the case of composites reinforced with high aspect ratio glass flakes (α=~150).

As mentioned earlier, high aspect ratio reinforcements are more effective in carrying loads as compared to low aspect ratio ones. However, incorporation of the high aspect ratio glass flakes results in a drastic decrease in the flexural strength leading to ~2.4 fold and ~3.7 fold reduction with respect to neat epoxy for the flake contents of ~76 vol% and ~78 vol%, respectively (Figure 6.a). The unexpected decline in the mechanical properties of the composites reinforced by highly aligned high aspect ratio glass flakes is thought to be arisen from the combined effect of microstructural features such as platelet cluster formation, void entrapment and flake fragmentation, along with the lack of bonding between the reinforcement and the epoxy matrix, as in the case of composites reinforced with glass platelets, all of which leads to either the formation of stress concentration sites or decrease in effective stress transfer from the matrix to the reinforcement. All these features (entrapped air voids, fragmented glass flakes and flake clusters) can be explicitly seen in Figure 5.

Furthermore, high aspect ratio glass flake incorporated composites exhibit lower flexural strength values than that of the composites reinforced by low aspect ratio glass platelets fabricated under identical processing conditions. Regardless of achieved well-alignment of the 2D building blocks along with the higher reinforcement aspect ratio and hence, higher stress transfer lengths, these lower flexural strength values are attributed to 20 vol% difference in the inorganic content, i.e. the size of the flake clusters along with the fraction of entrapped voids and fragmented flakes increases as the volume fraction of inorganic reinforcement increases. On the other hand, flexural strength value of ~76 vol% glass flake-epoxy matrix composite is comparable with that of the composite reinforced by 63 vol% glass platelets. Despite 13 vol% difference in the inorganic contents, this comparable flexural strength values is attributed to higher reinforcing efficiency of the high aspect ratio glass flakes.

On the contrary to flexural strength values, flexural moduli of the HASC processed composites, determined as 10±0.5 GPa and 6.9±0.9 GPa for the glass flake contents of ~76 vol% and ~78 vol%, respectively, are higher than that of the neat epoxy which is 2.4±0.1 GPa. Despite their higher inorganic content and higher reinforcement aspect ratio, composites reinforced with glass flakes provide comparable flexural modulus values with the glass platelet reinforced composites processed under the applied loads of 50 MPa and 100 MPa.

Stiffness of a composite is dependent on filler content, size and aspect ratio (α) besides the alignment of the fillers and the filler/matrix modulus ratio [50]. In the case of composites reinforced with glass platelets, increase in the flexural modulus with increasing reinforcement content followed by a decrease in it with further increase in the volume fraction of inorganic reinforcement reveals that there is an optimum matrix to reinforcement ratio in HASC processed nacre-mimetic bulk lamellar composites. Excessive drainage of the resin at hıgh processing pressures, and hence increase in the inorganic content of the composite via HASC processing beyond an optimum matrix to reinforcement ratio leads to a concomitant reduction in the effective aspect ratio for two reasons; (1) fragmentation of high aspect ratio glass flakes into two or more pieces, (2) enlargement of flake clusters, in which flakes are stacked together with insufficient epoxy between them. Furthermore, the lack of coupling and presence of voids at the interface also play a great role in the efficiency of rigid 2D fillers in restricting the deformation of the matrix. Therefore, in the case of composites reinforced with as-received flakes, dramatic reduction in the flexural modulus with the increase in the inorganic content from 76 vol% to 78 vol% is attributed to the combined effect of all above mentioned microstructural factors. The effect of these microstructural features are more pronounced in the case of composites reinforced with high aspect ratio glass flakes due to the fact that high aspect ratio glass flakes are more sensitive to fracture[51] and also they have greater tendency to form clusters.

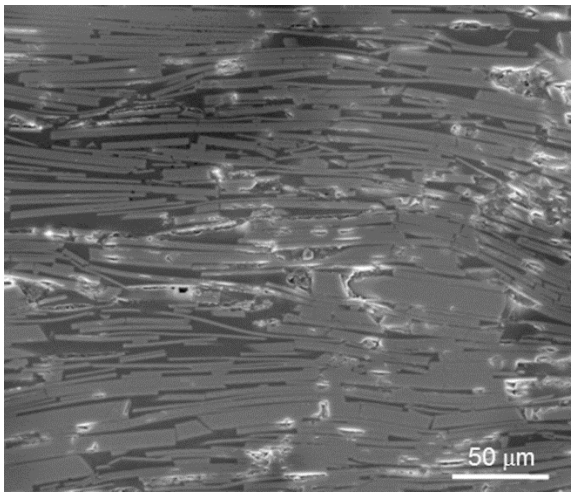

Figure 5 Cross-sectional microstructure of the GF-HASC 50 composite.

Fracture surface analysis of the HASC processed composite under the applied pressure of 100 MPa demonstrates that fracture occurs through the weak interface between glass flakes and the epoxy matrix leaving the flake surfaces clean and smooth (Figure 6.b). Furthermore, unlike glass platelet reinforced composites, for which after maximum stress failure occurs suddenly, for glass flake reinforced composites, following an increase up to the maximum, the stress decreases abruptly to some extent and then begins to decrease gradually (Figure 6.a). This observed tail behavior can be attributed to the higher aspect ratio of the reinforcement along with the governed fracture mode, i.e. high aspect ratio glass flakes continued to carry load until their embedded parts were completely pulled-out off the matrix leading to a slowly descending curve. All these findings pointing out that fracture is mainly governed by the flake pull-out rather than flake fracture, i.e. the aspect ratio of the glass flakes is lower than the critical aspect ratio for the glass flake reinforcement–EpoFix epoxy system. This finding is consistent with the aforementioned calculation performed to determine the

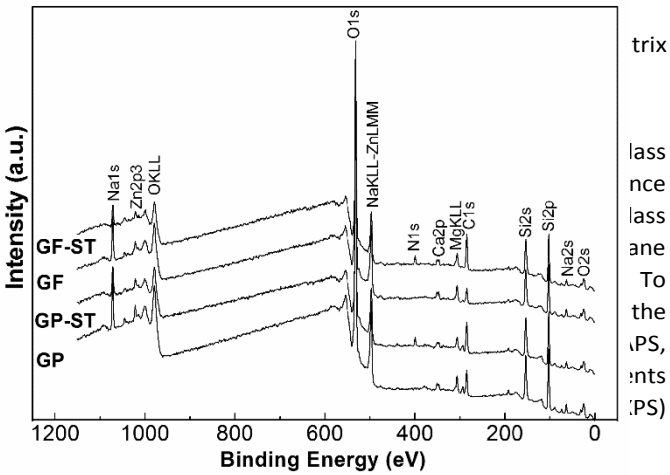

Figure **7** presents XPS survey spectra of APS treated and as-received glass platelets and flakes. Peaks at 25 eV, 63 eV, 89 eV, 103 eV, 154 eV, 285 eV, 293 eV, 347 eV, 532 eV, 1021 eV and 1072 eV are O2s, Na2s, Mg2s, Si2p, Si2s, C1s, K2p, Ca2p, O1s, Zn2p and Na1s peaks, respectively, where peaks at 306 eV, 498 eV and 978 eV correspond to MgKLL, NaKLL ZnLMM and OKLL Auger peaks. For APS treated platelets or flakes, XPS survey spectra show an additional peak corresponding to N1s. Presence of peaks other than Si, N, C and O peaks in the XPS spectra indicate that the thickness of the adsorbed silane layer is less than the analysis depth of XPS. Therefore, C, O and Si signals can be attributed to both silane layer adsorbed on the surfaces of the glass reinforcements and also to the glass reinforcement itself.

Silane coupling agents provide chemical linkage at the interface between two dissimilar materials such as inorganic reinforcement and organic matrix. For effective coupling at the interface, hydrolysable group of the silane molecule should react and make chemical bonds with the hydroxyl groups at the inorganic surfaces, whereas its organofunctional group should provide linkage with the organic phase.

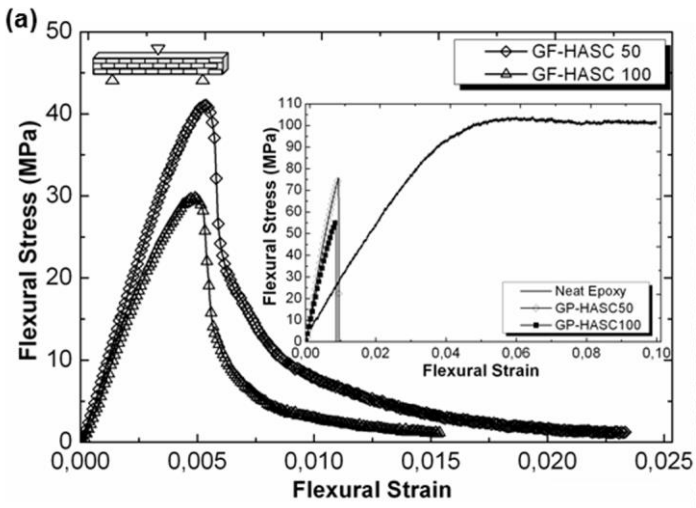

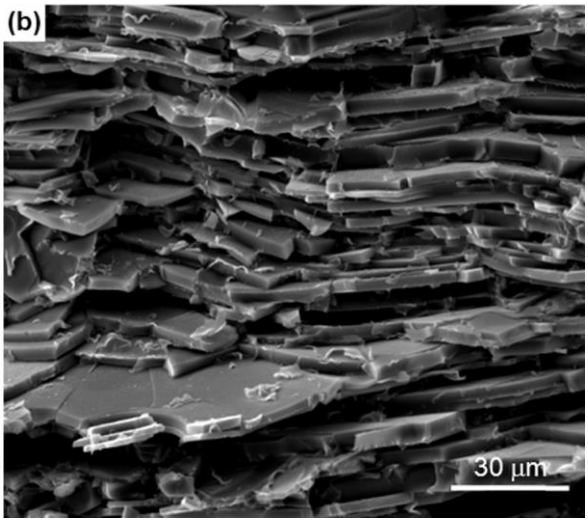

Figure 6 (a) Flexural stress-strain curves of glass flake reinforced composites (inset shows flexural stress-strain curves of glass platelet reinforced composites and neat epoxy) and (b) Fracture surface of GF-HASC 100 composite.

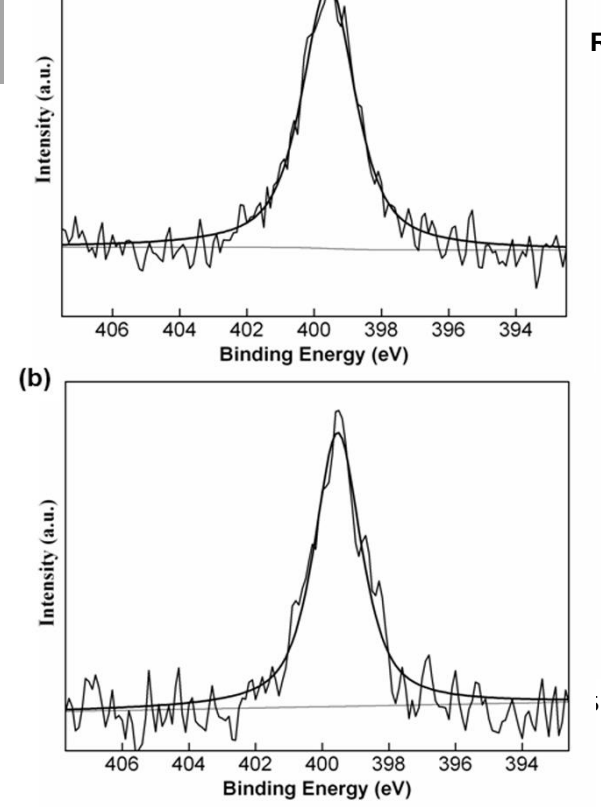

Figure **8**.b, respectively, are attributed to free NH_2 groups [56-58]. This indicates that the NH_2 groups of the silane molecules adsorbed on the surfaces of the 2D glass reinforcements are oriented towards the matrix side to provide linkage with the epoxy matrix.

3.4 Nacre-Mimetic Composites Reinforced by Surface Functionalized Glass Platelets or Flakes

Mechanical behavior of inorganic-organic composites is strongly affected by the properties of the interface between the reinforcement and matrix. Wettability and adhesion are important factors which control the effective load transfer from the matrix to the reinforcements, and hence play a crucial role in determining the overall mechanical performance of the material. For that reason, the surfaces of the glass reinforcements were treated with APS coupling agent.

Three-point bending test results, presented in **Error! Reference source not found.**, explicitly reveals the effect of interface adhesion on the flexural properties for both SM and HASC processed composites under the applied hot pressing pressure of 50 MPa and 100 MPa. Even in the case of the composite fabricated by simple mixing, reinforcing the epoxy matrix by APS treated glass platelets (GP-ST-SM) has led to significant improvement in mechanical properties resulting in ~40% and ~70% increase in flexural strength and flexural strain values, respectively, as compared to the composite reinforced by as-received platelets (GP-SM). For the composites HASC processed under the applied pressures of 50 MPa (GP-ST-HASC 50) and 100 MPa (GP-ST-HASC 100), more remarkable enhancement has been achieved, i.e. there is ~68% and ~100% increase in flexural strength values and this increase is accompanied by ~52% and ~44% enhancement in flexural strain values, respectively, when compared with HASC processed composites reinforced by as-received platelets (GP-HASC 50 and GP-HASC 100).

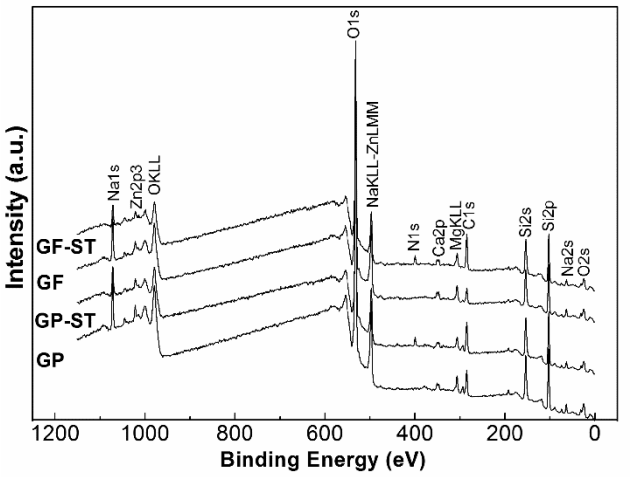

Figure 7 XPS spectra of APS treated glass platelets (GP-ST) and flakes (GF-ST) along with the spectra of as-received platelets (GP) and flakes (GF).

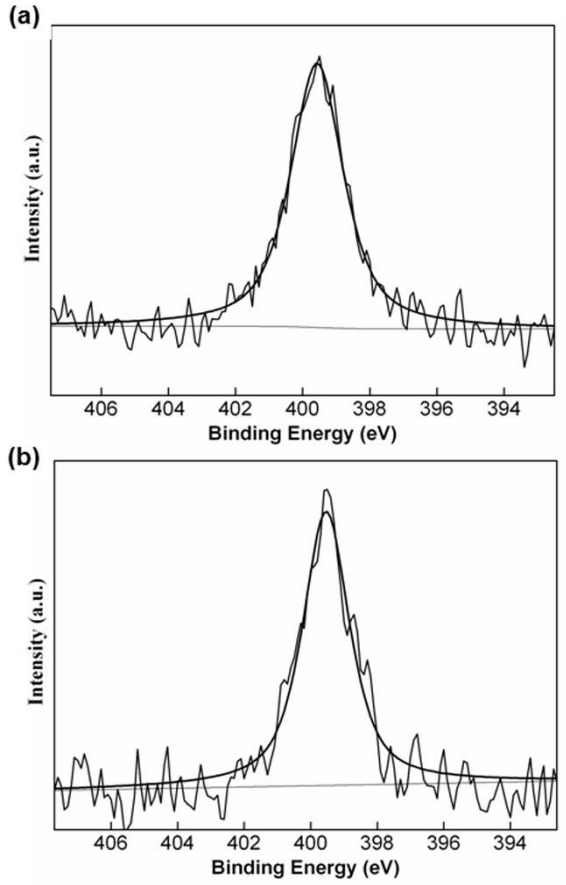

Figure 8 High resolution XPS spectra of N1s core level for APS treated (a) platelets (GP-ST) and (b) flakes (GF-ST).

Journal Name

ARTICLE

Table 2 Mechanical properties of the SM and HASC processed composites reinforced with either as-received or surface functionalized 2D glass reinforcements.

Designation	Hot Pressing Pressure (MPa)	Flexural Strength (MPa)	Failure Strain	Flexural Modulus (GPa)
GP-SM	0	80.8±2.1	0.02098±0.00151	4.3±0.1
GP-ST-SM	0	113.2±1.6	0.03566±0.00046	4.0±0.1
GP-HASC 50	50	77.6±2.6	0.00937±0.00022	9.9±0.2
GP-ST-HASC 50	50	130.1±2.5	0.01423±0.00064	11.7±0.3
GP-HASC 100	100	54.1±1.0	0.00868±0.00019	7.5±0.3
GP-ST-HASC 100	100	108.4±2.5	0.01249±0.00018	11.4±0.3
GF-HASC 50	50	43.3±3.1	0.02288±0.00085	10.0±0.5
GF-ST-HASC 50	50	69.1±1.1	0.02363±0.00071	14.5±0.5
GF-HASC 100	100	28.0±2.5	0.01611±0.00094	6.9±0.9
GF-ST-HASC 100	100	54.4±1.7	0.01738±0.00070	12.3±0.7

Furthermore, unlike the composites reinforced by as-received platelets, incorporation of surface treated glass platelets has led to an increase in flexural strength with respect to the neat epoxy. This increase is ~10% in the case of SM composite. With the increase in the glass platelet content and the improvement in the orientation of the glass platelets, this enhancement in flexural strength increases to ~26% for composite GP-ST-HASC 50. Nevertheless, further increase in the HASC processing pressure has not led to further improvement in flexural strength values. On the contrary, it has led to an improvement of only ~5%, which is lower than the improvement achieved in the case of the SM composite.

For the glass flake reinforced composites, the situation is similar to the composites reinforced by silane treated glass platelets, i.e. reinforcing the epoxy by surface treated high aspect ratio glass flakes has led to ~60% and ~95% improvement in the flexural strength values accompanied by a little improvement in the failure strain for HASC processed composites fabricated under the applied pressures of 50 MPa (GF-ST-HASC 50) and 100 MPa (GF-ST-HASC 100), respectively, as compared to composites reinforced by as-received flakes (GF-HASC 50 and GF-HASC100). However, it is clear that although silane treatment has led to significant improvement in flexural strength by increasing the effective load transfer between the matrix and the reinforcements, flexural strength values are still lower than the flexural strength of the neat epoxy. All these results indicate that microstructural features such as flake/platelet clusters, voids and fractured flakes/platelets also play a crucial role in determining the final mechanical properties of the composites as mentioned previously.

For the SM composite, reinforcing the epoxy with surface functionalized glass platelets does not impart extra stiffness when compared to SM composite reinforced by as-received glass platelets. On the other hand, the increase in the glass platelet content along with the improvement in the alignment of these glass platelets via HASC processing reveals the effect of surface treatment leading to ~18% and ~52% enhancement in stiffness for GP-ST-HASC 50 and GP-ST-HASC 100, respectively, with respect to the composite reinforced by as-received platelets.

The effect of silane treatment on flexural modulus is more pronounced in the case of composites reinforced by high aspect ratio glass flakes. The improvement in flexural modulus values are ~45% and ~78% for GF-ST-HASC 50 and GF-ST-HASC 100, respectively, as compared to the composites reinforced by as-received flakes. As aforementioned, stiffness of a composite is dependent on size and aspect ratio (α) beside the alignment of the reinforcements[50], the flexural modulus values for composites reinforced by either as-received glass platelets or flakes are on the same order. However, the composite reinforced by silane treated flakes has ~24% higher modulus value than the composite reinforced by silane treated glass platelets under the applied processing pressure of 50 MPa. This result clearly illustrates that coupling at the interface between the filler and the matrix also plays an important role in revealing the effect of the aspect ratio on the stiffness of the composites.

Figure 9 shows fracture surfaces of three-point bending (3PB) tested composites reinforced by APS treated platelets and flakes. Unlike the fractographs presented in Figure 4 and Figure 6 which demonstrate the presence of clean platelet surfaces indicating weak interfacial bonding between the platelets or flakes and the matrix, Figure 9 illustrates rough platelet and flake surfaces pointing out the effective adhesion of the epoxy to inorganic surfaces, and hence presence of an

effective chemical bonding between the glass reinforcements and the matrix. These micrographs also clearly indicate that for these composites main fracture mechanism is pull-out as in the case of composites reinforced by as-received reinforcements; however, in this case crack propagates through the matrix deflecting near the reinforcements rather than propagating through the platelet-matrix interface leaving their surfaces covered with epoxy.

Figure 10.a shows the load-displacement curves of SM and HASC processed composites reinforced by low aspect ratio glass platelets with SENB specimen geometry. Average WOF values, expressing the energy absorbed by a notched specimen until fracture per unit fracture surface area, were calculated as 115 J/m^2 and 110 J/m^2 for SM and HASC processed composites, respectively, both of which were reinforced by as-received glass platelets. These WOF values explicitly indicate that incorporation of glass platelets into epoxy matrix has led to considerable reduction in the WOF value of the neat epoxy which was calculated as 350 J/m^2.

Fracture behavior of the SM and HASC processed composites completely differs from each other demonstrating the fact that crack propagation was unstable leading to catastrophic failure for the SM composite, whereas for HASC processed composite crack propagation was stable as indicated by the tail behavior following the maximum in load-displacement curve. This tail behavior clearly indicates that main fracture, and hence energy absorption mechanism is platelet debonding and pull-out for the HASC processed composite.

Average WOF values of SM and HASC processed composites reinforced by silane treated platelets were calculated as 135 J/m^2 and 149 J/m^2, respectively. Although reinforcing the epoxy matrix by silane treated glass platelets has led to ~18% and ~49% enhancement in WOF values of SM and HASC processed composites, respectively, with respect to the composites reinforced by as-received platelets, WOF values are still lower than that of the neat epoxy.

Figure 10.b shows the load-displacement curves of composites reinforced by either as-received or silane treated high aspect ratio glass flakes along with the load-displacement curve of the neat epoxy. The composite reinforced by well-aligned as-received glass flakes exhibits considerably higher WOF value, which was determined as 221 J/m^2, as compared to composites reinforced by lower aspect ratio glass platelets. Along with the incorporation of surface treated flakes, WOF value is further improved (~31% higher than the WOF value of composite reinforced by as-received flakes).

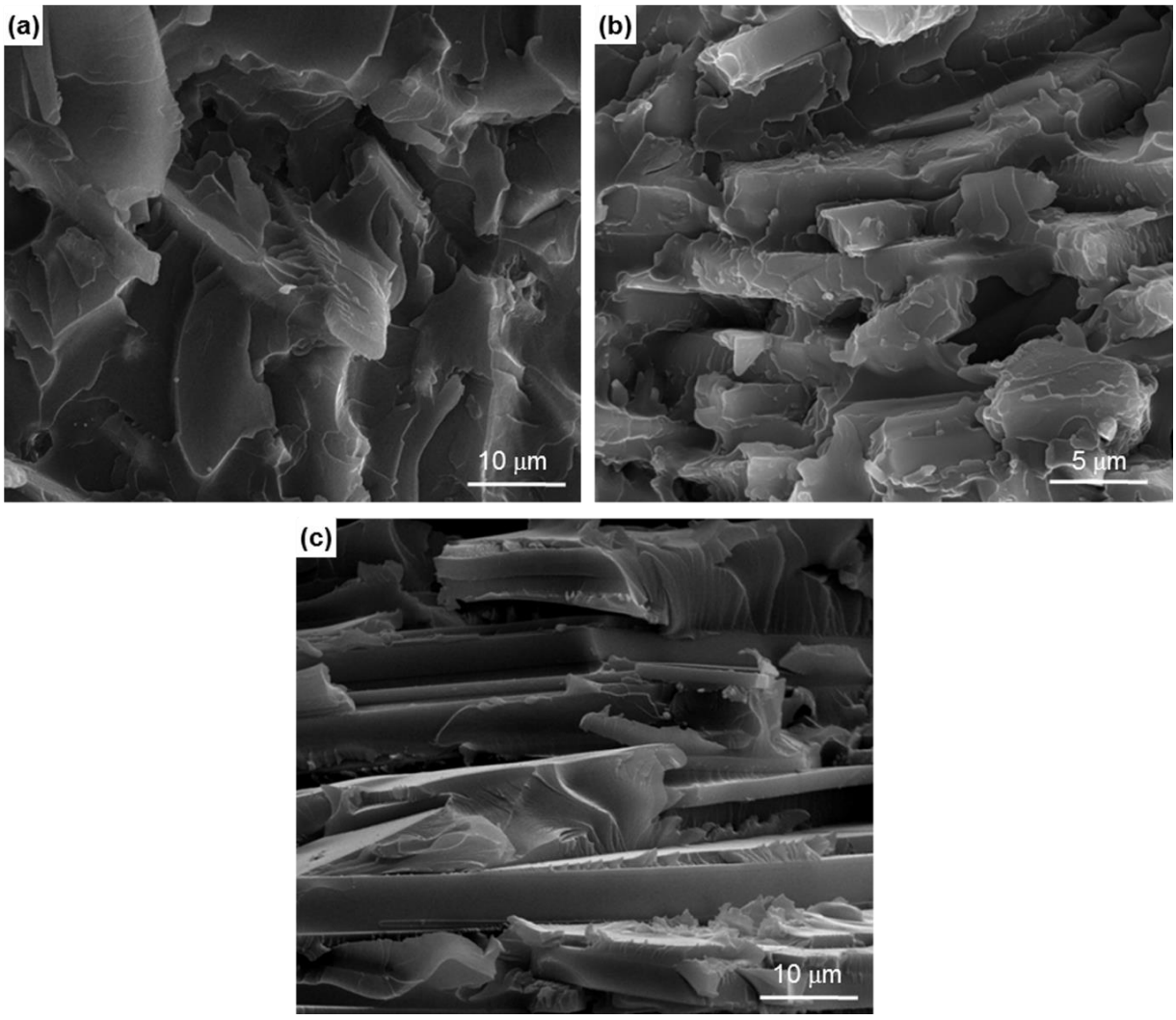

Figure 9 Fracture surfaces of 3PB tested specimens (a) GP-ST-SM, (b) GP-ST-HASC-50 and (c) GF-ST-HASC-50.

Journal Name

ARTICLE

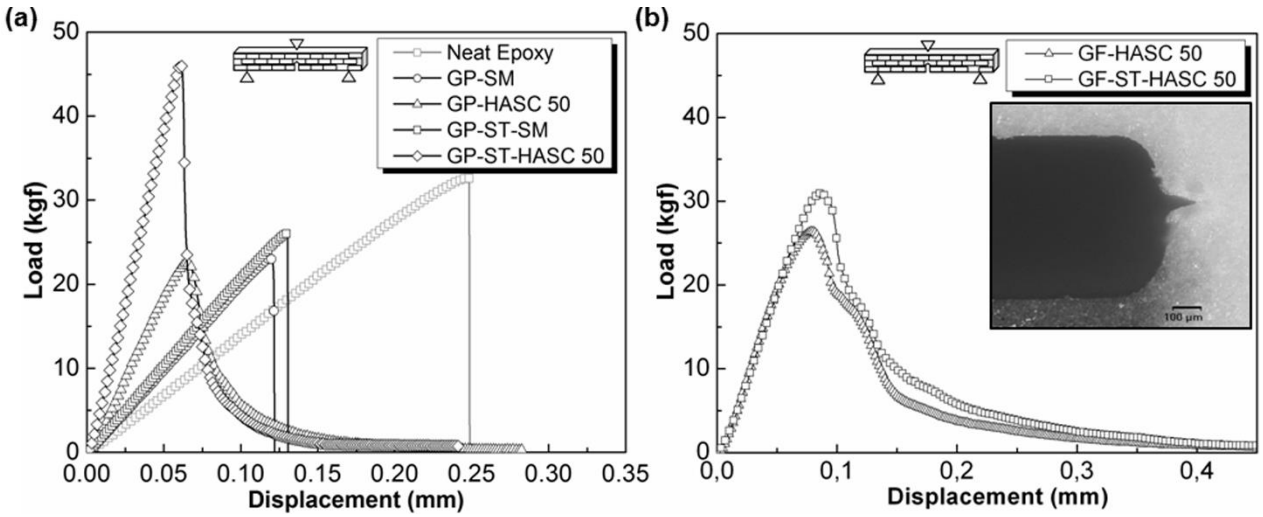

Figure 10 (a) Load-displacement curves of SENB specimens of SM and HASC processed composites either reinforced by as-received or surface functionalized platelets along with the load-displacement curve of the neat epoxy. (b) Load-displacement curves of SENB specimens of HASC processed composites reinforced by as-received or surface functionalized flakes (Inset shows optical microscope image of a typical notch and sharp pre-crack. Scale bar: 100 µm).

For the composites reinforced either by surface treated or as-received flakes, the tail behavior following the maximum in the load-displacement curve explicitly point outs stable crack growth. When Figure 10.a and Figure 10.b are compared it is clear that although fracture behaviors seem to be similar, composite reinforced by surface functionalized glass platelets exhibits a tail behavior after ~50% sudden decrease in the load, while the composite reinforced by surface functionalized high aspect ratio glass flakes reveals a tail behavior right after the maximum load.

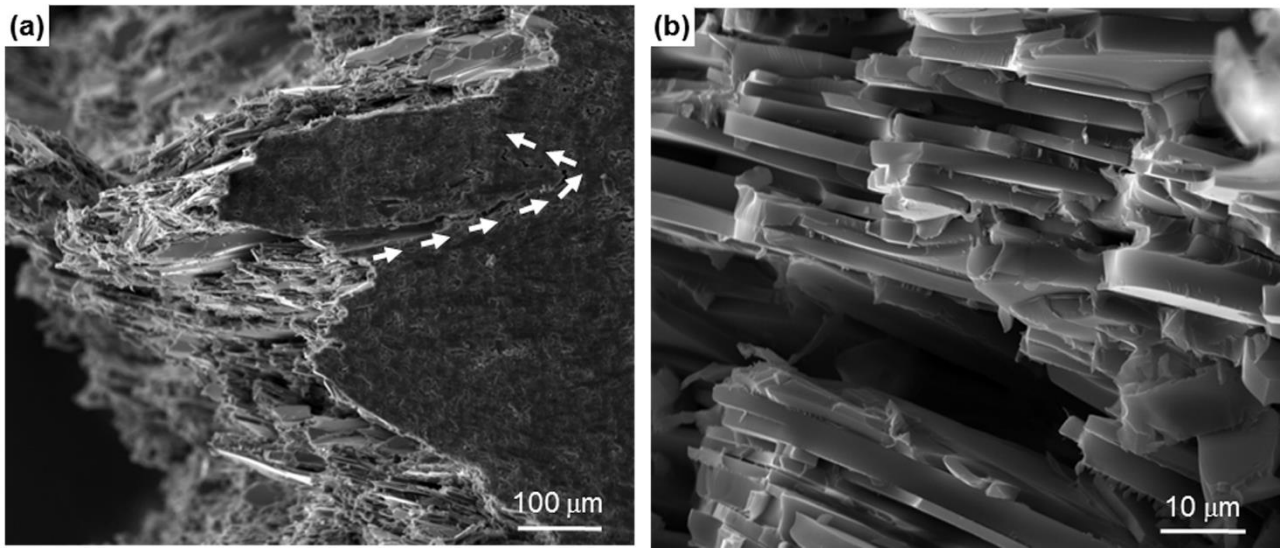

Figure 11 Fracture surface of the GF-HASC 50 WOF specimen.

Journal Name

ARTICLE

Fractographs of the WOF specimen of the GF-HASC 50 composite (Figure 11) clearly demonstrate that crack propagates through the weak as-received flake-matrix interface and continuously deflects around the well-aligned flake edges leaving the flake surfaces smooth and clean. The zigzag pattern of the crack leads to an increase in the crack path, and hence energy absorption, until fracture. The path of a secondary crack, shown in Figure 11.a, clearly illustrates extensive crack deflection exceeding a path length of 200 μm. Therefore, it can be deduced that flake debonding and crack deflection along with the flake pull-out lead to a tortuous crack path resulting in high work of fracture (WOF) values which can also be further improved by surface functionalization.

Conclusions

The novel HASC process is a one-step, easy, fast and scalable processing pathway that enables the fabrication of nacre-mimetic polymer matrix composites reinforced by well-aligned inorganic reinforcements of high volume fraction by draining the liquid resin and favoring 2D reinforcement orientation during processing. Therefore, with the use of this method, it is possible to fabricate organic matrix bulk composites with a lamellar microstructural architecture resembling to brick-and-mortar structure that of natural nacre.

Although, versatility of HASC processing allows fabrication of composites with wide variety of organic matrix-high strength inorganic reinforcement combinations, in the scope of this study, nacre-mimetic epoxy matrix composites reinforced by 2D glass reinforcements having different aspect ratios were fabricated. For both SM and HASC processed composites, regardless of the reinforcement aspect ratio, incorporation of as-received glass platelets or flakes has led to a drastic decrease in the flexural strength, yet an increase in the flexural modulus values with respect to neat epoxy. The decrease in flexural strength values could be attributed to combined effect of microstructural features such as platelet/flake cluster formation, void entrapment and platelet/flake fragmentation, along with the lack of bonding between the reinforcement and the epoxy matrix, all of which leads to the formation of stress concentration sites or decrease in effective stress transfer from the matrix to the reinforcement. The effect of these microstructural features on mechanical performance of the glass reinforcement-epoxy matrix composites has become more pronounced with the increase in the inorganic reinforcement content.

The coupling at the interface achieved through functionalization of the glass reinforcement surfaces with APS silane coupling agent leads to remarkable enhancement in mechanical properties by increasing the effective load transfer between the matrix and the reinforcements. In the case of composites reinforced by surface treated low aspect ratio glass platelets, achieved flexural strength values were higher than that of the neat epoxy. However, despite improved coupling at the interface and interfacial bonding between reinforcement and the matrix, flexural strength values of the composites reinforced by high aspect ratio glass flakes were still lower than that of the neat epoxy because of their high inorganic content. Nevertheless, for all composites, the fracture is governed by reinforcement pull-out mode, which maximizes the energy absorbed during fracture, rather than reinforcement fracture. Therefore, nacre-like brick-and-mortar structured composites reinforced by well-aligned high aspect ratio glass flakes exhibited high WOF values. For these composites, extensive crack deflection along with flake pull-out leads to highly torturous crack path similar to the crack growth behavior of natural nacre.

Notes and references

1. F. Barthelat, *Bioinspiration & Biomimetics*, 2010, **5**, 1-8.
2. D. K. Dubey and V. Tomar, *Annals of Biomedical Engineering*, 2010, **38**, 2040-2055.
3. A. P. Jackson, J. V. F. Vincent and R. M. Turner, *Proceedings of Royal Society B*, 1988, **234**, 415-441.
4. A. G. Evans, Z. Suo, R. Z. Wang, I. A. Aksay, M. Y. He and J. W. Hutchinson, *Journal of Materials Research*, 2001, **16**, 2475-2485.
5. R. Z. Wang, Z. Suo, A. G. Evans, N. Yao and I. A. Aksay, *Journal of Materials Research*, 2001, **16**, 2485-2493.
6. T. E. Schaffer, C. Ionescu-Zanetti, R. Proksch, M. Fritz, D. A. Walters, N. Almqvist, C. M. Zaremba, A. M. Belcher, B. L. Smith, G. D. Stucky, D. E. Morse and P. K. Hansma, *Chemistry of Materials*, 1977, **9**, 1731-1740.
7. F. Song, X. H. Zhang and Y. L. Bai, *Journal of Materials Research*, 2002, **17**, 1567-1570.
8. F. Song, A. K. Soh and Y. L. Bai, *Biomaterials*, 2003, **24**, 3623-3631.
9. M. A. Meyers, A. Y.-M. Lin, P.-Y. Chen and J. Muyco, *Journal of the Mechanical Behavior of Biomedical Materials I*, 2008, 76-85.
10. F. Barthelat, H. Tang, P. D. Zavattieri, C.-M. Li and H. D. Espinosa, *Journal of the Mechanics and Physics of Solids*, 2007, **55**, 306–337.
11. G. M. Luz and J. F. Mano, *Composites Science and Technology*, 2010, **70**, 1777-1788.
12. J. Sun and B. Bhushan, *RSC Advances*, 2012, **2**, 7617-7632.
13. V. Vertlib, M. Dietiker, M. Plötze, L. Yezek, R. Spolenak and A. M. Puzrin, *Journal of Materials Research*, 2008, **23**, 1026-1035.
14. L. J. Bonderer, A. R. Studart and L. J. Gauckler, *Science*, 2008, **319**, 1069-1071.

15. L. J. Bonderer, A. R. Studart, J. Woltersdorf, E. Pippel and L. J. Gauckler, *Journal of Material Research*, 2009, **24**, 2741-2754.
16. H. B. Yao, H. Y. Fang, Z. H. Tan, L. H. Wu and S. H. Yu, *Angewandte Chemie*, 2010, **122**, 2186 –2191.
17. W. Zhang, G. Xu, R. Ding, K. Duan and J. Qiao, *Materials Science and Engineering C*, 2013, **33** 99-102.
18. Y. Xu, W. Hong, H. Bai, C. Li and G. Shi, *Carbon*, 2009, **47**, 3538-3543.
19. X. Wang, H. Bai, Z. Yao, A. Liu and G. Shi, *Journal of Materials Chemistry* 2010, **20**, 9032-9036.
20. J. M. Malho, P. Laaksonen, A. Walther, O. Ikkala and M. B. Linder, *Biomacromolecules*, 2012, **13**, 1093−1099.
21. K. Shikinaka, K. Aizawa, N. Fujii, Y. Osada, M. Tokita, J. Watanabe and K. Shigehara, *Langmuir*, 2010, **26**, 12493-12495.
22. W. Zhu, C.-H. Lu, F.-C. Chang and S.-W. Kuo, *RSC Advances*, 2012, **2**, 6295-6305.
23. C. Aulin, G. Salazar-Alvarez and T. Lindstrom, *Nanoscale*, 2012, **4**, 6622-6628.
24. S. Korkut, J. D. Roy-Mayhew, D. M. Dabbs, D. L. Milius and I. A. Aksay, *ACS Nano*, 2011, **5**, 5214-5222.
25. R. Libanori, F. H. L. Münch, D. M. Montenegro and A. R. Studart, *Composites Science and Technology*, 2012, **72**, 435–445.
26. D. A. Kunz, J. Schmid, P. Feicht, J. Erath, A. Fery and J. Breu, *ACS Nano*, 2013, **7**, 4275–4280.
27. P. Das, S. Schipmann, J.-M. Malho, B. Zhu, U. Klemradt and A. Walther, *ACS Applied Materials and Interfaces*, 2013, **5**, 3738−3747.
28. E. Munch, M. E. Launey, D. H. Alsem, E. Saiz, A. P. Tomsia and R. O. Ritchie, *Science*, 2008, **322**, 1516-1520.
29. M. E. Launey, E. Munch, D. H. Alsem, H. B. Barth, E. Saiz, A. P. Tomsia and R. O. Ritchie, *Acta Materialia*, 2009, **57**, 2919-2932.
30. A. Dutta and S. A. Tekalur, *Materials and Design*, 2013, **46**, 802-808.
31. L. J. Bonderer, K. Feldman and L. J. Gauckler, *Composites Science and Technology*, 2010, **70**, 1958-1965.
32. L. J. Bonderer, K. Feldman and L. J. Gauckler, *Composites Science and Technology*, 2010, **70**, 1966-1972.
33. H. Kakisawa, K. Minagawa, S. Takamori and Y. Osawa, *Journal of the Ceramic Society of Japan*, 2005, **113**, 808-811.
34. H. Kakisawa, T. Sumitomo, R. Inoue and Y. Kagawa, *Composites Science and Technology*, 2010, **70**, 161-166.
35. Z. Q. Li, L. Jiang, G. L. Fan and D.Zhang, presented in part at the 18th International Conference on Composite Materials (ICCM-18), Jeju, South Korea, 2011.
36. R. M. Erb, R. Libanori, N. Rothfuchs and A. R. Studart, *Science*, 2012, **335**, 199-204.
37. R. Libanori, R. M. Erb and A. R. Studart, *ACS Applied Materials and Interfaces*, 2013, **5**, 10794−10805.
38. M. Xanthos, in *Functional Fillers for Plastics*, ed. M. Xanthos, WILEY-VCH Verlag GmbH & Co. KGaA, Weinheim, second edn., 2010, pp. 3-18.
39. S. N. Gurbuz and A. F. Dericioglu, *Materials Science and Engineering C*, 2013, **33**, 2011–2019.
40. P. Davies, A. Casinos, J. D. Currey and P. Zioupos, *Proceedings of the Royal Society B: Biological Sciences*, 2001, 107-111.
41. R. Rabiei, S. Bekah and F. Barthelat, *Acta Biomaterialia*, 2010, **6**, 4081–4089.
42. S. Zhao, J. Zhang, S. Zhao, W. Li and H. Li, *Composites Science and Technology*, 2003, **63**, 1009-1014.
43. C.-N. Wu, T. Saito, S. Fujisawa, H. Fukuzumi and A. Isogai, *Biomacromolecules*, 2012, **13**, 1927−1932.
44. J. Wang, Q. Cheng and Z. Tang, *Chemical Society Reviews*, 2012, **41**, 1111-1129.
45. E. Lokensgard, in *Industrial Plastics: Theory and Applications*, Delmar Cengage Learning, Canada, 5th Edition edn., 2010, ch. 7, p. 116.
46. A. N. Netravali, P. Schwartz and S. L. Phoenix, *Polymer Composites*, 1989, **10**, 385-388.
47. L. Onsager, *Annals of the New York Accademy Sciences*, 1949, **51**, 627-659.
48. R. A. L. Jones, in *Soft Coddensed Matter*, Oxford University Press, New York, 2002, pp. 122-126.
49. G. J. Vroege and H. N. W. Lekkerkerker, *Journal of Physical Chemistry*, 1993, **97**, 3601-3605.
50. M. Xanthos, in *Functional Fillers for Plastics*, ed. M. Xanthos, WILEY-VCH Verlag GmbH & Co. KGaA, Weinheim, second edn., 2010, pp. 19-42.
51. J. Lusis, R. T. Woodhams and M. Xanthos, *Polymer Engineering and Science*, 1973, **13**, 139-145.
52. D. I. Tee, M. Mariatti, A. Azizan, C. H. See and K. F. Chong, *Composites Science and Technology*, 2007, **67**, 2584-2591.
53. Y. Xie, C. A. S. Hill, Z. Xiao, H. Militz and C. Mai, *Composites: Part A*, 2010, **41**, 806-819.
54. H. Ishida, *Polymer Composites*, 1984, **5**, 101-123.
55. J. S. Quinton and P. C. Dastoor, *Surface and Interface Analysis*, 2000, **30**, 21-24.
56. A. S. M. Chong and X. S. Zhao, *Journal of Physical Chemistry B*, 2003, **107**, 12650-12657.
57. C. Perruchot, M. M. Chehimi, M. Delamar, E. Cabet-Deliry, B. Miksa, S. Slomkowski, M. A. Khan and S. P. Armes, *Colloid Polymer Science*, 2000, **278**, 1139-1154.
58. X. Liu, J. L. Thomason and F. R. Jones, *The Journal of Adhesion*, 2008, **84**, 322-338.

39x35mm (300 x 300 DPI)